Available online at www.sciencedirect.com
ScienceDirect
Journal of Nuclear Materials 373 (2008) 407–414
journal of nuclear materials
www.elsevier.com/locate/jnucmat

Prediction of TRISO coated particle performances for a one-pass deep burn

Alberto Talamo *

Nuclear Engineering Division, Argonne National Laboratory, 9700 S. Cass Ave, Argonne, IL 60439, USA

Received 26 August 2006; accepted 10 July 2007

Abstract

In the present studies, TRISO coated particle performances have been investigated for incinerating plutonium and minor actinides by the Gas Turbine-Modular Helium Reactor, whose fresh fuel is fabricated after the uranium extraction (UREX) process applied to Light Water Reactors irradiated fuel. The analyses divide into two parts: in the first part, the latest design of the reactor core proposed by General Atomics, which takes advantage of four fuel rings, has been modeled in deep details by the Monte Carlo MCNP code and a burnup process has been simulated by the MCB code. In the second part, the TRISO coated particle performances have been investigated by the PANAMA code with the goal of verifying the design constraints proposed by General Atomics. During burnup, the refueling and shuffling schedule followed the one-pass deep burn concept, where the fuel is utilized, since fabrication for the Gas Turbine-Modular Helium Reactor, without any reprocessing until the final disposal into the geological repository. During the reactor operation, the fast fluence on all TRISO particles layers has been evaluated and the production of the key fission products monitored. During an hypothetical reactor accident scenario, the TRISO particle failure fraction has been estimated.

1. Introduction

The Gas Turbine-Modular Helium Reactor (GT-MHR) [1], conceived by General Atomics (GA), has the capability to incinerate plutonium and minor actinides coming from the uranium extraction (UREX) process applied to Light Water Reactors (LWRs) irradiated fuel. Within this context, the plutonium and minor actinides burnup is often referred as 'deep burn' to emphasize that transuranic isotopes deplete more than 50%. In previous studies, two alternative scenarios have been investigated: the first one where the three years irradiated plutonium and minor actinides triple isotropic (TRISO) coated particles are reprocessed to manufacture fresh fuel TRISO coated particles (referred as two-pass deep burn to emphasize the reprocessing of the TRISO coated particles) [2] and the second one where the plutonium and minor actinides TRISO coated particles remain in the core until their final disposal into the geological repository (referred as one-pass deep burn to emphasize no reprocessing of the TRISO particles occurs) [3]; the two different options have shown transmutation rates of 94% and 83% for the key isotope ^{239}Pu. Since in both cases an accumulation of curium isotopes has been observed, the present studies focused on the transmutation of only neptunium, plutonium and americium by a one-pass deep burn. The major goal of the present analyses is the verification of the GA design constrains for the integrity of TRISO particles. Consequently, the analysis consists of two parts: in the first part the reactor burnup has been simulated by a Monte Carlo transport code and in the second part the results of the Monte Carlo transport code have been used as input in a thermo-chemical-mechanical code for evaluating TRISO coated particle performances.

2. The GT-MHR Monte Carlo modelling

The latest design of the GT-MHR, which exhibits four fuel rings, as shown in Fig. 1, has been described in a detailed 3D model by the Monte Carlo N-Particle (MCNP)

* Tel.: +1 630 252 2773.
E-mail address: alby@anl.gov

0022-3115/$ - see front matter © 2007 Elsevier B.V. All rights reserved.
doi:10.1016/j.jnucmat.2007.07.001

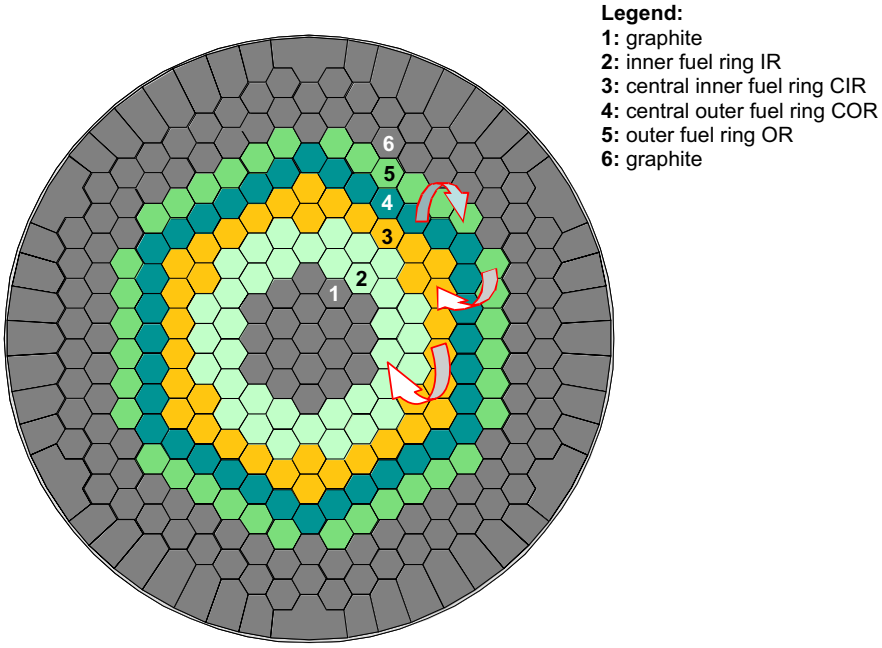

Fig. 1. Horizontal section of the GT-MHR core.

transport code [4]; that has cost a 5500–10 000 lines input (for the fresh and irradiated reactor core, respectively). Fig. 2 illustrates the fuel hexagonal block, which allocates 108 coolant channels and 216 fuel pins; the latter ones have been modeled as graphite cylinders filled by a body centered cubic lattice of TRISO particles. Fig. 5 of previous studies [2] illustrates the structure of the TRISO particles and their disposal inside the fuel pins, as represented in the Monte Carlo geometry model. Tables 1 and 2 report the geometry and material data, respectively, of the present core. In the present core configuration all control mechanisms (e.g. burnable poison or control rods) have been neglected.

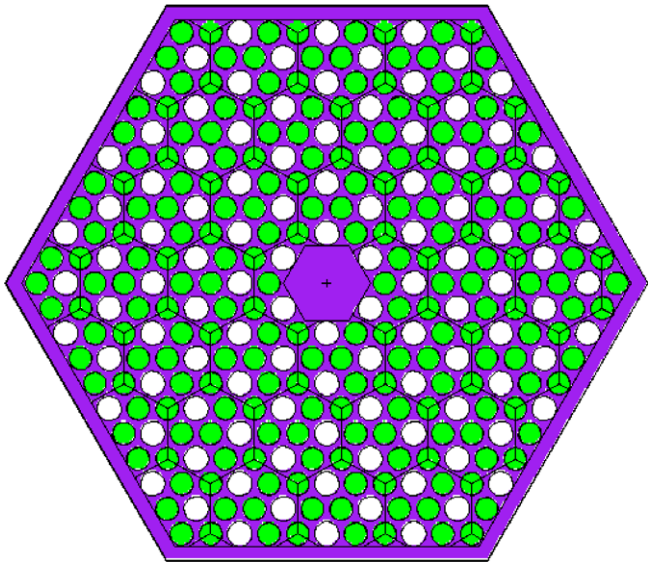

Fig. 2. Horizontal section of the fuel hexagonal block.

Table 1
Geometry data of the GT-MHR

Core-radius [cm]	385
Core-height [cm]	1030.885
Hexagonal fuel blocks – number	36×4
Hexagonal fuel blocks – apothem [cm]	17.9984
Hexagonal fuel blocks – height [cm]	793
Hexagonal fuel blocks – interstitial gap [cm]	0.1016
Hexagonal fuel blocks – fuel pins number	216
Hexagonal fuel blocks – coolant channels number	108
Hexagonal fuel blocks – fuel pins radius [cm]	0.6223
Hexagonal fuel blocks – fuel pins pitch [cm]	1.8796
Hexagonal fuel blocks – fuel pins hole radius [cm]	0.635
Hexagonal fuel blocks – coolant channel radius [cm]	0.79375
Hexagonal fuel blocks – fuel pins height [cm]	793
TRISO particles – kernel radius [μm]	100
TRISO particles – width porous graphite layer [μm]	150
TRISO particles – width inner pyrocarbon layer [μm]	35
TRISO particles – width SiC layer [μm]	35
TRISO particles – width outer pyrocarbon layer [μm]	40
TRISO particles – packing fraction [%]	20

The burnup calculation has been carried out by the Monte Carlo Continuous Energy Burnup MCB code [5–9], version 2 beta, which is an extension of the MCNP code; the MCB transport code has been equipped with a nuclear data library based on JEFF-3 and extended with: JENDL-3.3, ENDF\B-6.8 and DLC200, which has been used just for the evaluation of the scattering function $S(\alpha, \beta)$ of graphite. The Monte Carlo method allows to handle the triple heterogeneity of the GT-MHR without any spatial homogenization and to treat the neutron energy over a continuous domain; however, to reduce statistical fluctuations the number of simulated neutrons is so high that

Table 2
Material data of the GT-MHR

Isotope	Atomic density
Fuel $NpPuAmO_{1.7}$, $\rho = 10.36$ [g/cm^3], $T = 1500$ K	
^{237}Np	1.7198
^{238}Pu	0.49726
^{239}Pu	18.931
^{240}Pu	7.6878
^{241}Pu	2.7863
^{242}Pu	1.8131
^{241}Am	3.0262
^{242m}Am	0.011144
^{243}Am	0.55193
^{16}O	62.976
TRISO – porous carbon layer C, $\rho = 1$ [g/cm^3], $T = 1200$ K, $T_{S(\alpha,\beta)} = 1200$ K	
C	100
^{10}B	3.3163E−5
TRISO – pyrocarbon carbon layer C, $\rho = 1.87$ [g/cm^3], $T = 1200$ K, $T_{S(\alpha,\beta)} = 1200$ K	
C	100
^{10}B	3.3163E−5
TRISO – silicon carbide layer SiC, $\rho = 3.2$ [g/cm^3], $T = 1200$ K	
Si	50
C	50
^{10}B	1.6581E−5
Graphite C, $\rho = 1.74$ [g/cm^3], $T = 1200$ K, $T_{S(\alpha,\beta)} = 1200$ K	
C	100
^{10}B	3.3163E−5

the calculation has to be accomplished only by a computer cluster. Consequently, the MCB numerical simulations have been simultaneously performed on 10 AMD 64 bits processors, with a speed of 1800 MHz, and they required about 500 Mb of RAM memory per processor.

3. The one-pass deep burn

A total of 100 burnable material zones (regions of the core undergoing a different neutron flux intensity) has been simulated by the MCB code: 20 materials for the fuel in the TRISO kernels (for the fuel is disposed in the core into four rings and 10 axial zones, but the axial symmetry allows to use the same material both in the upper and lower zones) and four groups, each of 20 materials, for the four TRISO coated layers surrounding the fuel kernels (porous graphite, inner pyrocarbon, silicon carbide and outer pyrocarbon); this level of accuracy would have been impossible with the MONTEBURNS code, since it can handle only up to 50 burnable materials. The neutron flux in all burnable materials has been updated by MCB after the first 10 irradiation days, for taking into account the poisoning of the short life fission products, and thereafter after each 100 irradiation days until the total irradiation time reached a cumulative value of 300 days; thereafter, a natural decay of 30 days has been simulated to allow the refueling and shuffling operations. At the beginning of life (BoL), the 20 burnable zones corresponding to five fuel materials per ring are described below:

- inner ring: axial zones 1 2 3 4 5 5 4 3 2 1
- central-inner ring: axial zones 6 7 8 9 10 10 9 8 7 6
- central-outer ring: axial zones 11 12 13 14 15 15 14 13 12 11
- outer ring: axial zones 16 17 18 19 20 20 19 18 17 16

Materials 1, 6, 11 and 16 are disposed at the top and bottom of the core. After each irradiation period of 300 irradiation days, the radial shuffling applies the following operations:

- moving the fuel pins from the central-outer ring into the outer ring
- moving the fuel pins from the outer ring into the central-inner ring
- moving the fuel pins from the central-inner ring into the inner ring
- refueling the central-outer ring with fresh fuel
- discharging the fuel from the inner ring

Contemporaneously to the radial shuffling, the axial shuffling moves, for each ring, the fuel from the central zones into the outer ones and vice versa. For instance, after the first operational period, composed by 300 irradiation days and 30 natural decay days, the core configuration is rearranged as (see also Fig. 3):

- inner ring: axial regions 10 9 8 7 6 6 7 8 9 10
- central-inner ring: axial regions 20 19 18 17 16 16 17 18 19 20
- central-outer ring: axial regions fresh fuel
- outer ring: axial regions 15 14 13 12 11 11 12 13 14 15

At the end of the natural decay interval, the above refueling and shuffling schedule repeats, that sets the framework of the one-pass deep burn in-core fuel cycle (where the term 'in-core' indicates that the fuel cycle excludes

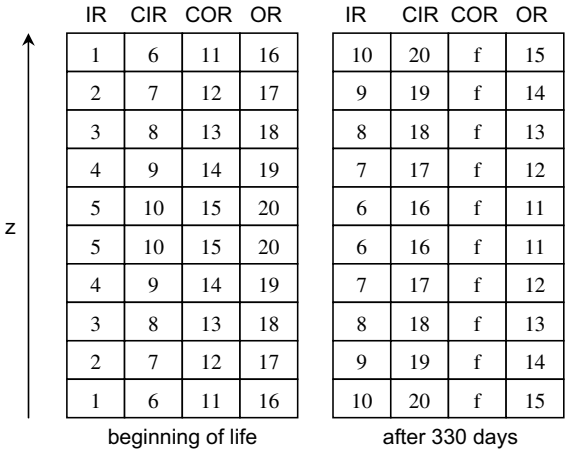

Fig. 3. Radial and axial shuffling operations after the first 330 days. f is acronym for fresh fuel.

extraction, manufacturing, reprocessing and final disposal into the geological repository phases).

4. Mechanisms of failure of TRISO particles

TRISO particles are composed by a central sphere containing the fuel and four concentric layers that are made of porous carbon, (inner) pyrocarbon, silicon carbide and (outer) pyrocarbon, respectively [10,11]. The porous carbon accommodates the gaseous fission products and CO; moreover, it allocates space for the kernel migration and swelling during irradiation. The inner pyrocarbon serves as smooth surface for the deposition of the SiC layer during the manufacture process and it delays the transport of fission products and of chlorine compounds to and from the SiC layer, respectively. The SiC layer is the major fuel cladding for it provides an impermeable barrier to the gaseous and metallic fission products. The outer pyrocarbon protects the SiC layer from mechanical damage during manufacture.

With the increase of the fast fluence, both the inner and outer pyrocarbon layers shrink and therefore they keep in compression the SiC layer (fuel cladding), which is dimensionally stable due to the very high elastic modulus of the silicon carbide; concurrently, the pressure of the fission gasses coming from the kernel induces a tensile stress on the SiC layer, but that is usually smaller than the compression strain [12,13]; consequently, the SiC layer remains intact provided that either, in the case the inner pyrocarbon layer remains undamaged, it remains in compression or, in the case the pyrocarbon cracks, the tensile stress does not exceed its strength. A TRISO particle failure may occur also in the inner pyrocarbon, which is simultaneously subject to both tensile stresses and compressive strains generated by the fission products gaseous pressure and the irradiation shrinkage, respectively [14]; in the tangential direction, the compressive strain always increases with fluence; whereas, in the radial direction the initial compressive strain changes into a tensile stress after a turnaround point that depends on the fluence value and the Bacon Anisotropy Factor (BAF); generally, a low BAF, indicating a more isotropic graphite, mitigates the strength of the forces acting on the pyrocarbon layers.

In addition, to the above mechanical mechanisms regulating the TRISO particle failure, there are also the thermo-chemical ones. In fact, the kernel can migrate up to the thermal gradient, the so called amoeba effect, that is caused by the solid state diffusion of carbon to the cooler side of the kernel and that produces an immediate particle failure when the kernel touches the SiC layer. Moreover, the noble metal fission products (e.g. Ru, Rh, Pd and Ag) may chemically attack the SiC layer [15,16]. Furthermore, in an accident scenario, if the fuel temperature exceeds 2000 °C, the SiC rapidly decomposes; however, the previous process begins to occur, at slower rates, already above 1700 °C [17,18]. The production of CO has multiple deleterious effects on the TRISO particles starkness since it increases the pressure of the gaseous fission products, it facilitates the amoeba effect and the corrosion of the SiC layer.

Table 3
GA design parameters of TRISO coated particles [19]

Parameter	Maximum	Average
Fuel temperature [°C] (normal operation)	1350	1000
Fuel temperature [°C] (accident conditions)	1600	–
FIMA [%]	90	80
Fast fluence [10^{21} n/cm^2]	8	6
Irradiation days	1300	1300
Allowable fuel failure Fraction	4E−4	4E−4

The fission products may also be partially released by intact particles; in fact, the outlet temperature of the coolant is limited to 850 °C because of the deposition in the primary coolant circuit of ^{110m}Ag; inter alia, the latter nuclide, together with ^{137}Cs, is the major contributor to the operators dose.

The integrity of TRISO particles results from all the previously listed failure mechanisms and it depends on many parameters, amid them the fuel temperature (at normal and accident conditions), the burnup (measured in fissions per initial fissile metal atom, FIMA), the fast fluence (of neutrons with an energy higher than 0.18 MeV) and the cumulative irradiation time. Table 3 reports the above-mentioned design parameters and the allowable fuel failure fraction according to the current GA fuel design [19]. Finally, the replacement of SiC with ZrC would provide a better performance of the TRISO particles from the point of view of the thermo-chemical resistance [20–23].

5. Calculation of the fast fluence and FIMA

The calculation of the fast fluence required the manipulation of a matrix 500×200, coming from 100 materials $\times$ 5 time steps $\times$ 100 energy groups (for each energy group the matrix contained both the energy bin and neutron spectrum data); the matrix has been extracted from the BMES output file of the MCB code which tallies the neutron flux by 100 energy groups for each burnable material (accordingly, the fast fluence threshold has been set to 0.2 MeV). Figs. 3 and 4 plot, at the equilibrium of the fuel composition, the fast fluence averaged in the TRISO kernel and in the porous carbon layer, respectively. During the first 300 irradiation days, the fresh fuel in the kernels starting at position 11 (axial outer region and central-outer ring) undergoes a lower intensity of the fast fluence, due to neutron leakage and to the moderation of the axial reflector. The opposite occurs for the fresh fuel in the kernels starting at position 15 (axial central region), which experiences a harder neutron spectrum. At 300 irradiation days, the above phenomenon produces in the axial central region a fast fluence value 1.9 higher than the value in the axial outer region. Each 300 irradiation days, the previous trend reverts due to the upside down axial shuffling. The fast fluence averaged in the intermediate positions in-between the

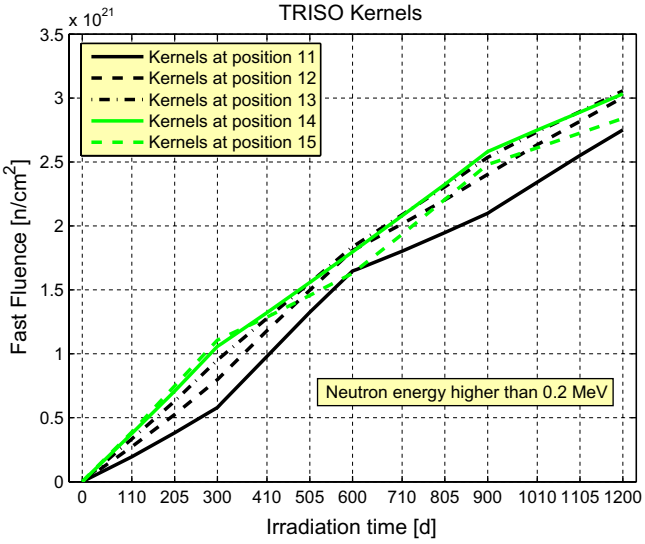

Fig. 4. Fast fluence, averaged in the TRISO particles kernel, as function of the cumulative irradiation time.

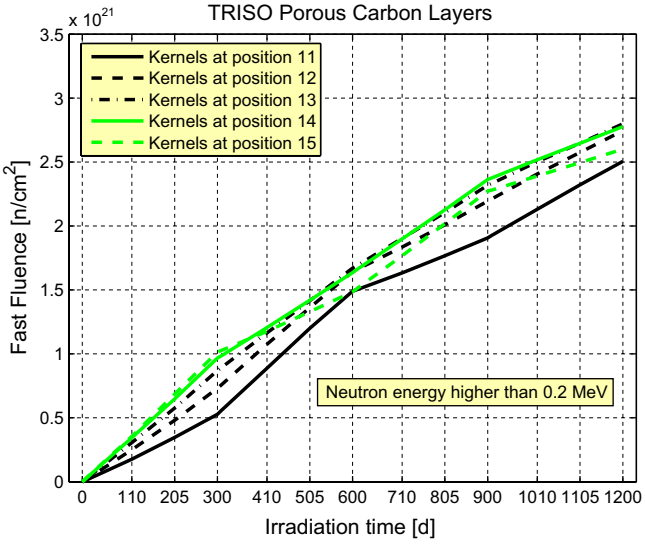

Fig. 5. Fast fluence, averaged in the TRISO particles porous carbon layer, as function of the cumulative irradiation time.

central and the outer axial regions exhibits a smoother change of slope compared to those ones for the kernels at positions 15 and 11. At the end of life, the kernels at the latter positions experienced the lowest value of the fast fluence. Of course, the fast fluence in the fuel (TRISO kernels) results larger than in the fuel cladding (TRISO coated layers); however, all values never exceed the threshold of 3.05×10^{21} n/cm^2, a value that well satisfies the GA constraints (Table 3). The time evolution of the fast fluence averaged in the other TRISO particles layers resembles the profiles illustrated in Fig. 5 for the porous carbon layer; therefore, further plots have been omitted.

The fission per initial metal atom (FIMA) has been approximated by Eq. (1)

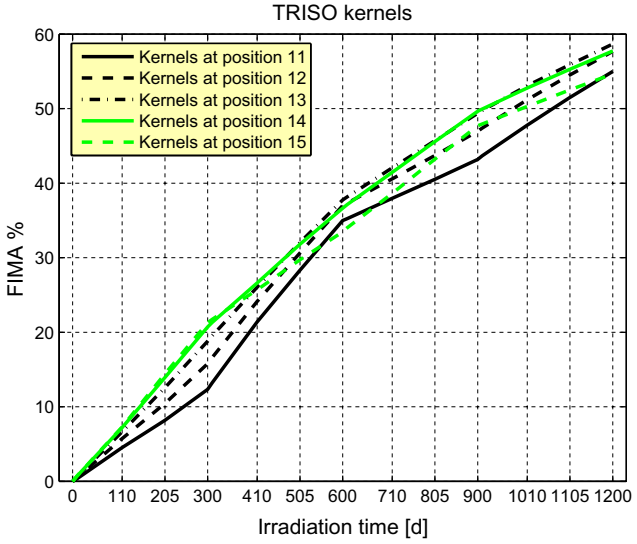

Fig. 6. FIMA as function of the cumulative irradiation time.

$$\begin{aligned}\mathrm{FIMA}(t) &= \frac{\text{number of fissions}}{\text{initial number of heavy metal atoms}} \\ &= \frac{\text{initial number of heavy metal atoms} - \text{number of heavy metal atoms}}{\text{initial number of heavy metal atoms}} \\ &\approx \frac{MA_0 - MA(t)}{MA_0}, \end{aligned} \tag{1}$$

where $MA(t)$ and MA_0 are the actinides masses at times t and 0, respectively. The evolution of the FIMA with time has been sketched in Fig. 6; at first glance, it is plain visible that the slopes of the FIMA follow those ones of the fast fluence so that all the previous remarks hold. However, the profiles of the fast fluence are driven by the fast part of the neutron spectrum, whereas most the fissions occur in the thermal and epithermal energy ranges. At the end of life, the FIMA of the central region (position 15) equals the value in the outer region (position 11) due to the compensating effect of the upside down axial shuffling.

The destruction of 55–59% of the actinides obtained by a one-pass deep burn in-core fuel cycle, obtained in the present studies, could be enhanced by a two-pass deep burn; however, TRISO coated particles reprocessing could be difficult due to the toxicity of the minor actinides, especially curium.

6. Calculation of the key fission products evolution

The analysis of the burnup results has shown that ruthenium is mainly composed by isotopes 100, 101, 102 (the most abundant), 104, 103 and 106; the first four are stable isotopes, whereas ^{106}Ru and ^{103}Ru transmute, via β-decay with a half-life of 373.6 and 39.26 days, into ^{106}Rh and ^{103}Rh, respectively. The latter stable nuclide is the major contributor to rhodium. Palladium is mainly composed by isotopes 104, 105 (the most abundant), 106, 108, 110 and 107, all are stable isotopes (but the latter one, which β-decays into ^{107}Ag with a half-life of 6.5 millions of years). Krypton is mainly composed by isotopes 82, 83, 84, 86 (the

most abundant) and 85, the first four are stable isotopes and the latter transmutes into ^{85}Rb, via β-decay with a half-life of 10.76 years. Xenon is mainly composed by isotopes 128, 129, 130, 131, 132, 134 and 136 (the most abundant), all are stable nuclides (but the latter one, which β-decays into ^{136}Cs with a half-life longer than 2.3×10^{21} years). Fig. 7 sketches the evolution of the mass of Ru, Rh, Pd, Kr and Xe, for the kernels starting at position 11, as function of the cumulative irradiation time (the natural decay intervals have been omitted); at 300, 600 and 900 irradiation days the mass is sampled after irradiation and before the axial and radial shuffling (the initial mass before irradiation, after the shuffling and natural decay interval has been omitted). The remarks discussed in the previous section concerning the axial shuffling for the fast fluence and the FIMA hold also for the noble metal and gaseous fission products. The diminishing of ruthenium at 310, 610 and 910 irradiation days is due to the decay of ^{103}Ru; of course, the latter process drives also the increase the rhodium mass. At the end of life, the mass of xenon results 32 times larger than that of krypton and the mass of ruthenium results 4.8 and 1.57 times larger than the one of rhodium and palladium, respectively.

Fig. 8 illustrates the evolution of ^{110m}Ag, ^{137}Cs, ^{134}Cs, ^{154}Eu, ^{155}Eu and ^{125}Sb for the kernels starting at position 11; none of these fission products is stable, since they transmute, via β-decay, into ^{110}Cd, ^{137}Ba, ^{134}Ba, ^{154}Gd, ^{155}Gd and ^{125}Te with a half-life of 249.8 days, 30.07, 2.06, 8.59, 4.76 and 2.76 years, respectively. We monitored these key fission products since their release has been experimentally measured for coated particles fuelled with uranium [16]; however, a comparison with the experimental results is not possible because of the different fission products yield of plutonium and minor actinides compared to uranium. Moreover, the fission products relative abundance is strongly dependent on the irradiation time, fuel composition and neutron flux spectrum. Amid the selected fission products, the cesium isotopes are the most abundant, especially ^{137}Cs; whereas, ^{110m}Ag represents the smallest contributor.

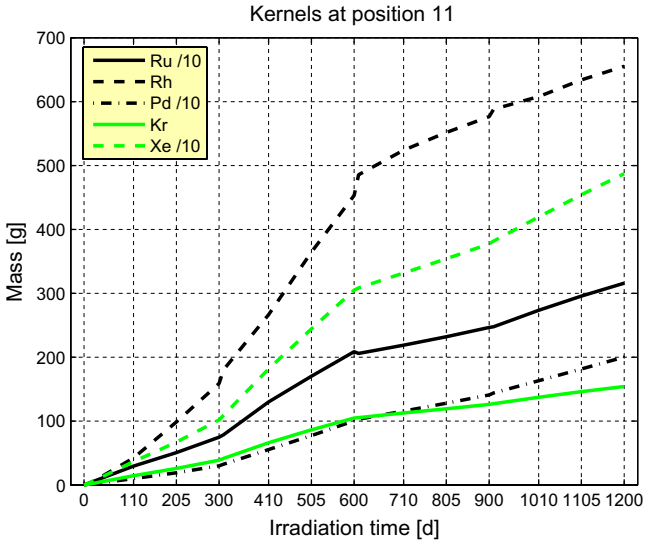

Fig. 7. Accumulation of Ru, Rh, Pd, Kr and Xe as function of the cumulative irradiation time. The masses of Ru, Ph and Xe have been divided by a factor 10.

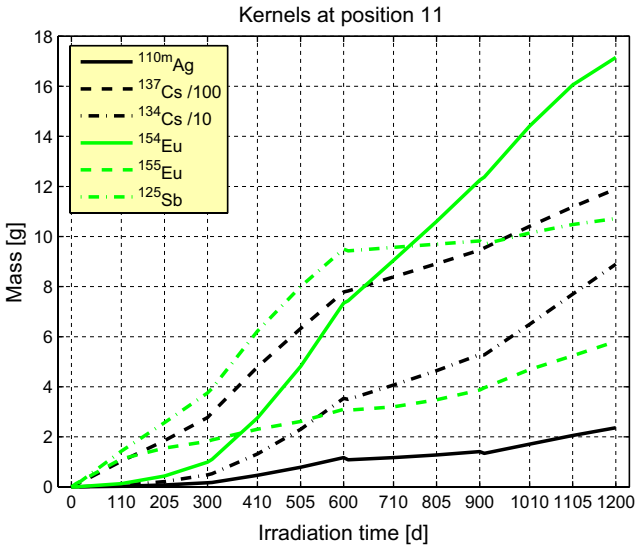

Fig. 8. Accumulation of ^{110m}Ag, ^{137}Cs, ^{134}Cs, ^{154}Eu, ^{155}Eu and ^{125}Sb as function of the cumulative irradiation time. The mass of ^{137}Cs and ^{134}Cs has been divided by 100 and 10, respectively.

7. Calculation of the failure fraction

The calculation of the failure probability of the coated particles in an accident scenario has been carried out by the PANAMA thermo-chemical-mechanical code [24]; the original FORTRAN source files, written for a DEC ALPHA architecture, have been modified to be exported on a Linux environment. The code allows only the utilization of three fuel types, ThO_2, UCO and UO_2; therefore, the latter fuel has been used and two small changes in the program source code have been applied:

- The fuel volume per mole has been changed from 24.38 to 25.74 cm^3/mol to take into account the larger mass of the $NpPuAmO_{1.7}$ fuel compared to UO_2.
- The oxygen production per fission event has been decreased by 15% to take into account of the smaller stoichiometric ratio of $NpPuAmO_{1.7}$ fuel compared to UO_2.

In the PANAMA code, the CO formation process followed the experimental law found by Proksch et al. [25]; the validity of the former law for the $NpPuAmO_{1.7}$ fuel is a topic open for further studies. The theoretical law describing the CO formation proposed by General Atomics [19] neglects the irradiation temperature and therefore has not been considered in the present studies. The experimental data for the reduced diffusion coefficient of fission gases in the $NpPuAmO_{1.7}$ kernel material are not available and

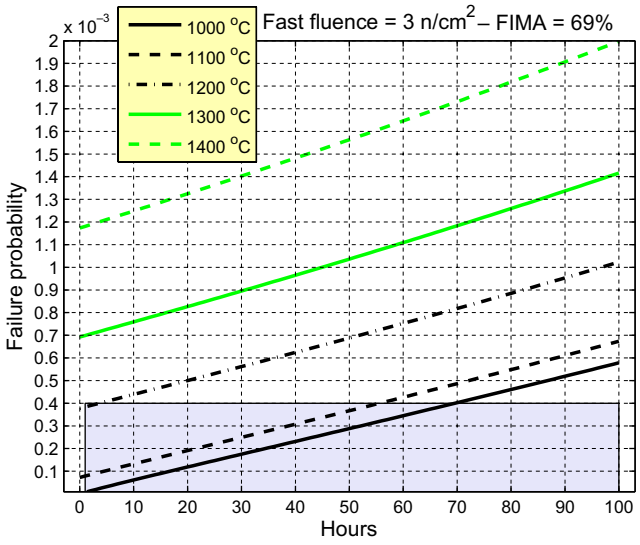

Fig. 9. TRISO particles failure probability as function of time after and accident scenario that sets a constant temperature of 1600 °C. The irradiation temperature during the 1200 irradiation days previous to the accident has been assumed constant and equal to 1000, 1100, 1200, 1300 or 1400 °C. The shadowed area marks the GA constrain of 4E−4.

therefore they have been approximated by the data for UO_2. In all the PANAMA calculations, the corrosion of the SiC layer has been neglected.

During all the 1200 irradiation days, a constant irradiation temperature has been assumed, with values equal to 1000, 1100, 1200, 1300 or 1400 °C. After 1200 irradiation days, an accident scenario that sets a constant temperature of 1600 °C for 100 h has been assumed. The failure fraction strongly depends on the SiC strength and Weibull modulus of the SiC layer. In the present studies we assumed the SiC strength and the Weibull modulus equal to 722 MPa and 7, respectively (Table 3.3 of Ref. [24]). During the 1200 irradiation days, when the irradiation temperature is 1000 °C, the SiC strength and Weibull modulus diminish down to 624.74 MPa and 5.63, respectively. Before the accident scenario, the PANAMA code calculated 0.16 or 0.625 oxygen atoms per fission event for an irradiation temperature of 1000 or 1400 °C, respectively. Fig. 9 illustrates the TRISO particle failure probability according to the irradiation temperature during the first 100 h of the accident scenario. It plain appears that if the irradiation temperature exceeds 1100 °C, then all TRISO particles may fail already at the beginning of the accident. TRISO particles maintain their integrity for 50–70 h provided that the fuel temperature during the normal operation and the accident scenario keeps below 1000–1100 and 1600 °C, respectively.

8. Conclusions

The level of the fast fluence in the TRISO coated particles depends on the local position of the fuel in the core. Axial outer regions due to leakage and the moderation of the axial reflector experience lower values. After an irradiation of 1200 irradiation days, the maximum value of the fast fluence is 3.05×10^{21} n/cm^2; at the same time, the FIMA is about 59%.

In the $NpPuAmO_{1.7}$ fuel, ruthenium represents the largest contributor to the noble metals fission products and xenon represents the largest contributor to the gaseous ones. A comparison with experimental results for ^{110m}Ag, ^{137}Cs, ^{134}Cs, ^{154}Eu, ^{155}Eu and ^{125}Sb obtained in previous studies for a uranium fuel is not possible because of the different fission product yields.

In the present studies it has been found that TRISO particles can maintain their integrity for 50–70 h at a constant temperature of 1600 °C provided that the irradiation temperature during burnup does not exceed 1000–1100 °C.

The incineration of plutonium and minor actinides from LWRs irradiated fuel in a one-pass deep burn in-core fuel cycle requires experimental measurements for the material properties of the SiC layer (strength and Weibull modulus).

Moreover, the description of the TRISO coated particle behavior by the PANAMA code could be improved if experimental data for the reduced diffusion coefficient of fission gases in the kernel material and the CO formation law for the $NpPuAmO_{1.7}$ fuel would be available.

Acknowledgements

Special thanks to Professor Gudowski, Chair Professor of the Reactor Physics Department of the Stockholm Royal Institute of Technology (Sweden), for allowing the utilization of the computer cluster and to Drs Verfondern and Nabielek, from the Jülich Research Center (Germany), for helping in understanding the PANAMA code features.

References

[1] General Atomics, GT-MHR conceptual design description report, GA/NRC-337-02, 2002.
[2] A. Talamo et al., Ann. Nucl. Energy 31 (2) (2004) 173.
[3] A. Talamo, W. Gudowski, Nucl. Sci. Eng. 156 (2) (2007) 244.
[4] J.F. Briesmeister, A general Monte Carlo N-Particle transport code – version 4c, LANL, LA-13709-M, 2002.
[5] J. Cetnar et al., MCB: a continuous energy Monte Carlo burnup simulation code, in actinide and fission product partitioning and transmutation, EUR 18898 EN, OECD/NEA 523, 1999.
[6] J. Cetnar et al., in: Proc. Accelerator Application 2001 and ADTTA 2001 Nuclear Application in the New Millennium, Reno, USA, 2001.
[7] J. Cetnar, Ann. Nucl. Energy 33 (7) (2006) 640.
[8] A. Talamo, W. Gudowski, J. Cetnar, Ann. Nucl. Energy 33 (7) (2006) 653.
[9] A. Talamo et al., Ann. Nucl. Energy 33 (14–15) (2006) 1176.
[10] H. Nickel et al., Nucl. Eng. Des. 217 (2002) 141.
[11] K. Sawa et al., Nucl. Eng. Des. 208 (2001) 305.
[12] K. Sawa, T. Tobita, Nucl. Technol. 142 (2003) 250.
[13] K. Sawa et al., J. Nucl. Sci. Technol. (2001) 411.
[14] G.K. Miller et al., J. Nucl. Mater. 295 (2001) 205.
[15] K. Minato et al., J. Nucl. Mater. 202 (1993) 47.
[16] K. Minato et al., Nucl. Technol. 131 (2000) 36.
[17] K. Fukuda et al., Nucl. Eng. Des. 157 (1995) 221.
[18] H. Nabielek et al., Nucl. Technol. 84 (1989) 62.

[19] M.B. Richards, R.K. Luu, Design of Coated Particles Driver and Transmutation Fuels, GA-224-0-RDE-000135 Rev. A, 2002.
[20] K. Minato et al., J. Nucl. Mater. 252 (1998) 13.
[21] K. Minato et al., J. Nucl. Mater. 249 (1997) 142.
[22] K. Minato et al., J. Nucl. Mater. 279 (2000) 181.
[23] K. Minato et al., Nucl. Technol. 130 (2000) 272.
[24] K. Verfondern, H. Nabielek, PANAMA Ein Rechenprogramm zur Vorhersage des Partikelbruchanteils von TRISO-Partikeln unter Störfallbedingungen, Jül – Spez – 298, ISSN 0343-7639, 1985.
[25] E. Proksch, A. Strigl, H. Nabielek, J. Nucl. Mater. 136 (1985) 129.